6-2011

Detecting ice-sheet melt area over western Greenland using MODIS and AMSR-E data for the summer periods of 2002–2006

Matthew F. McCabe
University of New South Wales, mmccabe@unsw.edu.au

Petr Chylek
Los Alamos National Laboratory

Manvendra K. Dubey
Los Alamos National Laboratory

Remote Sensing Letters
Vol. 2, No. 2, June 2011, 117–126

Taylor & Francis
Taylor & Francis Group

Detecting ice-sheet melt area over western Greenland using MODIS and AMSR-E data for the summer periods of 2002–2006

MATTHEW F. McCABE*†‡, PETR CHYLEK§ and MANVENDRA K. DUBEY†
†Earth and Environmental Sciences, Los Alamos National Laboratory, Los Alamos, NM 87545, USA
‡School of Civil and Environmental Engineering, University of New South Wales, Sydney, NSW 2052, Australia
§Space and Remote Sensing, Los Alamos National Laboratory, Los Alamos, NM 87545, USA

(*Received 9 March 2010; in final form 7 June 2010*)

We present the results from two independent approaches for monitoring ice-sheet melt area over western Greenland. The microwave-based cross-polarization gradient ratio (XPGR) approach (Abdalati, W. and Steffen, K., 1995, Detecting ice-sheet melt area over western Greenland using MODIS and AMSR-E data for the summer periods of 2002–2006. *Geophysical Research Letter*, **22**, pp. 787–790) is compared with a newly developed technique that exploits reflectance characteristics of snow/ice using near-infrared and visible wavelengths, to assess the extent of ice-sheet melt area over the west coast of Greenland. Data from the moderate resolution imaging spectroradiometer (MODIS) sensor onboard the National Aeronautics and Space Administration's (NASA) Earth Observing Satellite (EOS) Terra are analysed through the years 2002–2006 to monitor melt area extent between May and September. Concurrently, the XPGR ratio is derived from advanced microwave scanning radiometer (AMSR-E) data to develop a comparative measure of melt area over the same period of investigation. Although the techniques represent fundamentally different physical approaches, good agreement is observed between these distinct melt area products. The enhanced spatial resolution that is achieved from the MODIS sensor offers additional insight into the melt response over the course of the summer melt period and highlights the advantage of synthesizing diverse sensors and retrieval algorithms for Earth observation.

1. Introduction

Remote observations of the Greenland ice sheet have detected decreasing ice-sheet mass (Velicogna and Wahr 2006), accelerating outflow of ice (Ringot and Kanagaratnam 2006) and increasing regions of summer melt area (Abdalati and Steffen 1997, Mote 2007, Hall *et al.* 2009). Although a variety of remote sensing approaches have been employed to assess the mass exchange over the ice sheet, the resulting mass balance exhibits a wide range of scatter because of limited spatial and temporal sampling, measurement errors and coarse resolution, resulting in considerable uncertainty in quantifying the net mass flux over the Greenland ice sheet (Cazenave 2006). Consequently, there is a need for both accurate monitoring of ice

*Corresponding author. Email: mmccabe@unsw.edu.au

Remote Sensing Letters
ISSN 2150-704X print/ISSN 2150-7058 online
http://www.tandf.co.uk/journals
DOI: 10.1080/01431161.2010.501830

sheets as a whole, including regions bordering ice-sheet margins where accelerated melting and outflow has been observed, and also the advancement of high spatial resolution modelling of the ice-sheet dynamical responses. Current ice-sheet models lack the capacity to characterize recent changes observed over the Greenland and West Antarctic ice sheets, so improved observational constraints are required.

One of the essential parameters needed to monitor the status of the ice sheet is the extent of summer melting area. An empirical approach that has been developed to fill this gap is the cross-polarization gradient ratio (XPGR) (Abdalati and Steffen 1995). The XPGR uses differences in microwave brightness temperatures at 19 and 37 GHz resulting from emissivity changes as ice melts (Ulaby *et al.* 1982) to infer a transition between the dry and melting snow. Although XPGR has been shown to provide useful insight into the melt dynamics over the Greenland ice sheet using extensive records of the scanning multi-channel microwave radiometer (SMMR) data (Abdalati and Steffen 2001, Fettweis *et al.* 2007), which operated from 1979 to 1987, its coarse resolution limits its application for high-resolution modelling assessments. The same is true for scatterometer data that have also been used to efficiently map melt extent over the Greenland ice sheet (Nghiem *et al.* 2005) using data from the National Aeronautics and Space Administration's (NASA) Quick Scatterometer (QuickScat) satellite. Retrieval of melt area with a higher spatial resolution than the currently available 625 km^2 (25km $\times$ 25 km) would prove very useful in providing mechanistic insights into understanding cryospheric dynamics and improving modelling applications.

Algorithms recently developed to distinguish between water, ice and mixed-phase clouds (Chylek and Borel 2004) using near-infrared wavelengths provide a starting point for the development of a satellite-based method for the detection of snow melt area. Here we present a comparison of the XPGR approach with a recently developed algorithm based on moderate resolution imaging spectroradiometer (MODIS) data, for monitoring the melt area of the Greenland ice sheet (Chylek *et al.* 2007). Although the techniques represent physically different approaches and sense over different wavelengths and depths, considerable consistency is observed. This illustrates that although the approaches are distinct, they offer commensurate means of determining melt area and provide independent characterizations of melt dynamics over the Greenland ice sheet.

2. Data and methodology

A region along the west coast of the Greenland ice sheet, extending from 67°N to 76°N, formed the focus area for this study (see figure 1). Imagery obtained from MODIS on NASA's Earth Observing Satellite (EOS) Terra and the Aqua-based Advanced Microwave Scanning Radiometer (AMSR-E) sensor for the summer melting period of 1 May to 30 September were compiled for analysis using the data available since the launch of the AMSR-E satellite in mid-2002. A summary of the sensor characteristics pertinent to this investigation is included in table 1. AMSR-E data have the capacity to retrieve melt area estimates every day, irrespective of most atmospheric conditions (although it will be affected by precipitation). MODIS detections, on the contrary, are constrained to clear-sky retrievals because of atmospheric attenuation of visible and near-infrared wavelengths. In compiling the MODIS record, only the most cloud-free image was retained for each day, even though multiple images are often available to provide overlapping geographic coverage

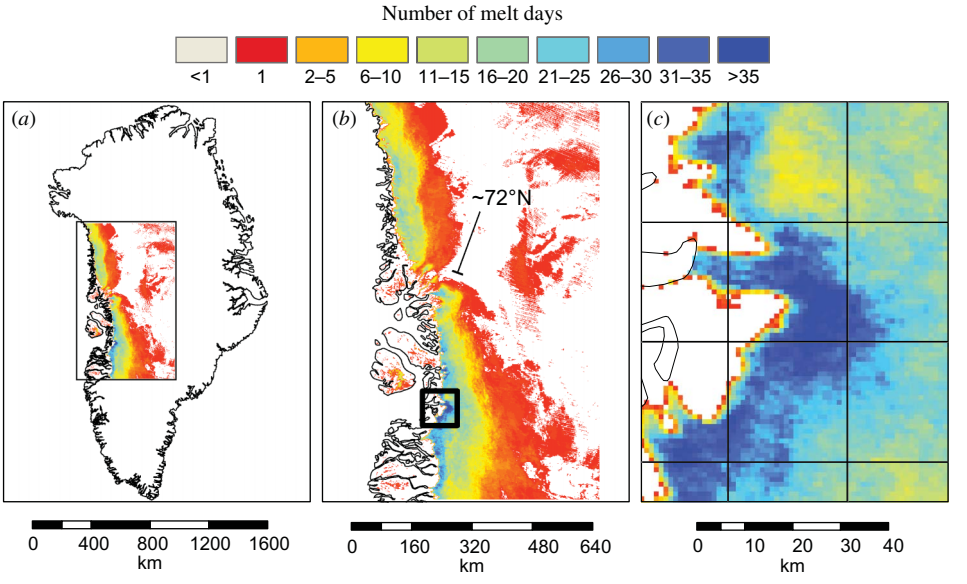

Figure 1. (*a*) Location of study area over the central western portion of the Greenland ice sheet; (*b*) MODIS melt area extent for the period of 1 May to 30 September 2005; and (*c*) overlay of the 25-km AMSR-E grid with respect to the high-resolution MODIS retrieval (right). Jakobshavn Isbrae Glacier, identified by the boxed region in (*b*) and enlarged in (*c*), illustrates the advantage of the high-resolution detail and spatial variability in MODIS imagery relative to the single AMSR-E pixel value (black grid lines) that would be retrieved using the XPGR alone.

Table 1. Comparison of AMSR-E and MODIS sensor characteristics.

Sensor satellite		Record length[a] (days)	Spectral bands	Resolution	Measurement depth
AMSR-E Aqua	2002	89	19 GHz	25 km × 25 km	2 cm at 19 GHz[b]
	2003	154			
	2004	155			
	2005	155	37 GHz		8 cm at 37 GHz[b]
	2006	153			
MODIS Terra	2002	129	620–670 nm	1 km × 1 km[c]	>40 μm[d]
	2003	137	2105–2155 nm		
	2004	123			
	2005	136			
	2006	123			

Notes: [a]MODIS records indicate number of days for which imagery was used, not clear-sky conditions.
[b]From Ulaby *et al.* (1986) and Abdalati and Steffen (1997) assuming a volumetric liquid water content >2%.
[c]MOD02 reflectance data are also available at 500 m resolution.
[d]The minimum thickness of surface water that can be sensed by the MODIS approach, derived in part from skin-depth calculation formulated in Jackson (1975).

(as both satellites are in sun-synchronous, near-polar orbits, the proximity of the study area to the polar region ensures the possibility of multiple overpasses each day).

On average, there were approximately 150 days of available AMSR-E imagery for each year, excluding 2002 when there were only 89 due to sensor outages and data unavailability. MODIS retrievals are limited by cloud cover issues, meaning that a temporally continuous record of melt cannot be produced. Although the MODIS records are not evenly spaced in time, clear-sky days were relatively evenly distributed throughout the whole study period.

2.1 *The cross-polarization gradient ratio*

The XPGR takes advantage of the difference in polarizations between the 19 and 37 GHz channels to discriminate melting from non-melting pixels:

$$\mathrm{XPGR} = \frac{T_{\mathrm{B,19H}} - T_{\mathrm{B,37V}}}{T_{\mathrm{B,19H}} + T_{\mathrm{B,37V}}}, \tag{1}$$

where T_{B} is the microwave brightness temperature in the 19 GHz horizontal polarization ($T_{\mathrm{B,19H}}$) and 37 GHz vertical polarization ($T_{\mathrm{B,37V}}$). Using the 25-km Level 3 Sea Ice Product (AE_SI25), the XPGR ratio was derived using the 18.7 and 36.5 GHz channels. Although this XPGR ratio is not completely equivalent to the original SMMR formulation, it is not anticipated that significant error will result from these differences. A melt threshold value of –0.025 was employed based on similar analysis using the special sensor microwave imager (SSM/I) data (Abdalati and Steffen 1995), although alternative threshold values have been used (Abdalati and Steffen 2001). AMSR-E pixels determined to exceed the XPGR threshold were accumulated throughout the study period to produce a composite map of melt area.

2.2 *Melt area detection index*

Although there are a number of functionally similar approaches that make use of band ratios to identify snow cover and extent, including the normalized difference snow index of Hall *et al.* (2002), the MODIS-based melt area detection index (MADI) represents an improved capacity to distinguish between snow morphology, using reflectance characteristics to discriminate between dry and melting snow as opposed to just distinguishing between snow-covered and snow-free pixels. We define the MADI as follows:

$$\mathrm{MADI} = \frac{R_{0.67}}{R_{2.1}}, \tag{2}$$

where $R_{0.67}$ is the reflectance in the MODIS band 1 (620–670 nm) and $R_{2.1}$ is the reflectance in band 7 (2105–2155 nm). A full physical description and validation of the approach is described in Chylek *et al.* (2007).

Using reflectance values from MOD021KM data, a collection of MODIS imagery was compiled over the summer melting months between 1 May and 30 September. A threshold value of MADI > 65 was used to indicate melting snow, based on previous analysis using high-resolution multispectral thermal imaging (MTI) data (Chylek *et al.* 2007). Values below this empirically determined threshold can potentially be discriminated further into cloud, dry ice and snow-free pixels, although we do not explore that capacity here. In developing seasonal melt area maps, the MADI was calculated for every pixel in the daily MODIS imagery. Each pixel that satisfied the

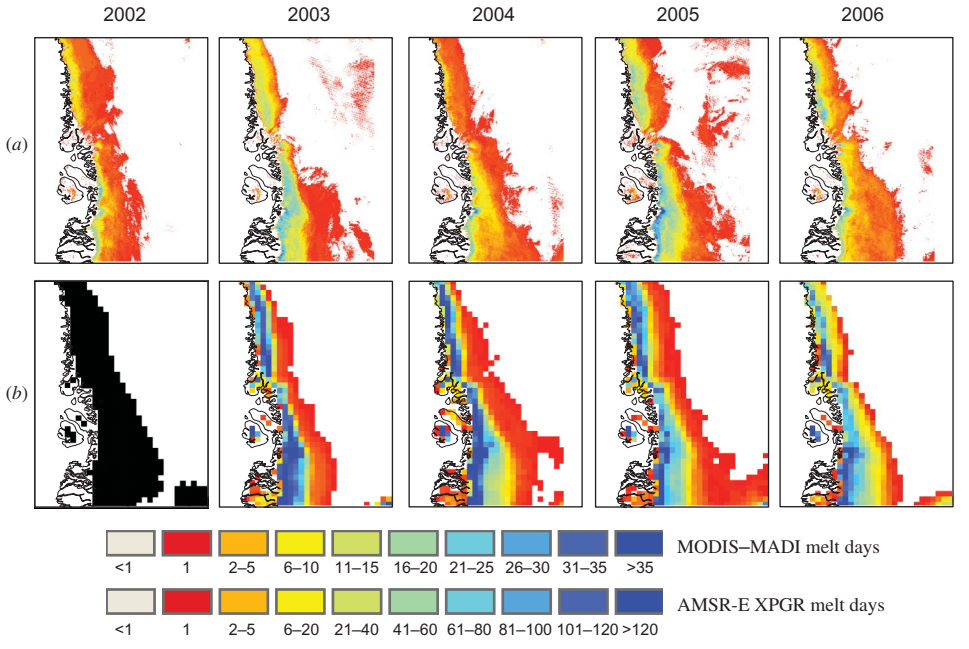

Figure 2. (*a*) Comparison of MODIS melt area extent using the MADI index and (*b*) AMSR-E-derived XPGR melt area for the central western portion of the Greenland ice sheet over the summer melting period from 1 May to 30 September. As AMSR-E retrievals for 2002 were unavailable for the full period, only melt extent is shown, as depicted in black.

MADI criteria (MADI $>$ 65) was characterized as melting and subsequently summed across all available imagery to produce a cumulative melt area map.

When graphically comparing these melt indices, different time scales are necessary because MODIS does not retrieve melt information under cloudy conditions, resulting in a varying number of available data through the melting season. Although the same colour scale is used in comparing the data (see figure 2), the melt period corresponding to these is different. The colour scale used here partitions the data into multi-day increments of melting pixels. In MADI retrievals, dark blue areas correspond to pixels that melt for greater than 35 days of the available MODIS data, with other days either not-melting or having the surface obscured by cloud. The same dark blue region in the AMSR-E imagery corresponds to pixels where the number of melt days is greater than 130 (from a total of 155 AMSR-E images for 2004; see table 1). In all cases, red regions indicate where pixels are detected to be melting for a single day only through the available observations. No empirical equivalence between the different melt-day approaches is assumed, with the scales used purely for comparative purposes. As 2002 represented a data limited year (AMSR-E imagery was not available until mid-June) and thus is inconsistent with the remaining years, only the area of melt extent is compared with MODIS–MADI retrievals.

3. Results and discussion

3.1 *High-resolution results from MODIS–MADI*

Although constrained by atmospheric conditions, one of the key advantages of the MODIS–MADI approach is the higher resolution that is obtained for melt area

characterization. As can be seen in figure 1, the spatial variability evident in the MODIS scene for the 2005 melt season is considerable. Total melt days calculated from the available MODIS data indicate the highest melt rates along the coastal fringe, extending 15–30 km inland (blue region) and representing consistent pixel melt through the available clear-sky imagery for that year. An advantage of higher resolution retrievals is the reduction of the influence of mixed pixel response, particularly along the sea/land/ice boundary and also for cases when only a fraction of a sensed pixel might be undergoing melt. A single AMSR-E melt response represents an area of 625 km^2 region compared to a 1 km^2 MODIS-based estimate, offering an enhanced capacity for mapping melt heterogeneity – particularly along the coastal fringe.

To highlight the spatial insight available through the application of the MADI approach, a boxed region outlined in figure 1(*b*) locates the Jakobshavn Isbrae Glacier, Greenland's largest outlet glacier and the focus of a number of recent studies investigating increased glacial acceleration and outflow (Thomas *et al.* 2003, Joughin *et al.* 2004). Comparisons of retrievals at the resolution of typical microwave-based retrievals (gridded lines in figure 1(*c*)) illustrate the improved characterization of both spatial structure and melt response resolved from the higher resolution MODIS approaches.

3.2 *Comparison of the spatial patterns of the MADI- and XPGR-derived melt areas*

Figure 2 details the MADI and XPGR retrievals for the years 2002–2006. The melt season of 2005 was determined in independent analysis to have been a record in terms of both melt area and maintenance of melting pixels over the entire Greenland ice sheet using microwave data (Steffen and Huff 2005). Likewise, 2002 was determined to have the next largest amount of melt from the then 24-year record of microwave-based observations (Steffen *et al.* 2004). From figure 2, the MODIS analysis, while supporting the greater amount of melting in 2005, does not indicate that 2002 was notably different from other years – at least over this small portion of the Greenland ice sheet. In this region, the overall areal extent of the melt for the study region seems to remain relatively consistent across the 5 years of satellite data. However, the spatial distribution and variability of melt appear to change notably between the individual years.

All years, and 2003 and 2005 in particular, reflect the elevation influence on the melt response. Across the image, distinct regions of melt match well with local elevation, as is expected. The 2000-m contour, which has previously served as an arbitrary threshold of interior melt advance in this region, provides a relatively consistent boundary delineating melt progression. The influence of elevation can be seen clearly around latitude 72°N (see figure 1) where a region of increased elevation is reflected in a lack of melt response in that area.

Some consistency with the analysis of Steffen and Huff (2005) is present in the detection of interior melt above the 2000-m elevation contour as displayed in figures 1 and 2 for the year 2005. Recent analysis of the 2007 summer period (Tedesco *et al.* 2008) using SSM/I retrievals indicated a record for melting above 2000 m elevation in south-western Greenland. In comparing the MODIS- and AMSR-E based approaches here, there are regions of interior melt that are detected by MADI in 2003 and 2005, which are not replicated in the AMSR-E imagery, either in this XPGR analysis or in the retrievals of Steffen and Huff (2005). These apparent inconsistencies highlight the need for additional examination of different

melt-detection approaches, the thresholds used in these and also a more careful analysis of *in situ* and model data to assess the level of cross-platform and source consistency.

Although overall melt-area extent provides a clear indicator of inter-annual variability, an equally informative feature in assessing melt response is the spatial pattern of melt, particularly as an indicator of changing melt dynamics on the ice sheet. In terms of the transition from coastal to inland region melting, figure 2 identifies clear similarities for MADI retrievals in the years 2003 and 2005, despite representing quite different overall areal extents. Interestingly, these spatial patterns of melt, particularly within 100 km of the coast, are less pronounced in other MODIS–MADI retrievals. Whether this reflects an actual reduction in the number of melt days during this period or is a result of the intermittent nature of retrievals from MODIS requires further investigation. It is the variability between coastal to inland melting that represents perhaps the key difference between the MODIS and AMSR-E retrievals analysed here. AMSR-E data display a relatively consistent response of near-coastal melt through all years, with 2006 indicating the least amount of sustained coastal melting (0–50 km) excluding 2002 due to the lack of an equivalent temporal range of data. Indeed, if 2005 represented a year of record melt area, 2006 would seem to represent a year of reduced melt duration – at least along the coastal-inland margin (0–100 km). In the XPGR data, 2003 and 2004 stand out as examples of increased near-coastal melt (in terms of number of melt days) rather than 2005. Whether these trends are regional in nature, explaining their divergence from analyses which have examined the melt response over all of Greenland (e.g. Hanna *et al.* 2005), or represent actual differences between the two approaches can only be determined through additional analysis of MODIS data encompassing all land areas. Examining correlation of melt regions with coastal-temperature data (Chylek *et al.* 2007, Mote 2007), sea-ice concentration (Rennermalm *et al.* 2009) or regional climate model output (Tedesco *et al.* 2008) may provide further insight into the cause of these inter-annual spatial variations.

Irrespective of the variations between the two approaches, there is considerable spatial agreement between the two products. Close inspection of the data illustrates greater spatial variability in the MODIS data, particularly around the coastal fringe (see figure 1) – but this is somewhat expected due to the higher resolution. In 2003 and 2005, there is considerably more structure evident in the MADI than is possible to retrieve using the coarser resolution AMSR-E. As noted above, the MODIS imagery reflects the distinct melting regimes across the study region: regimes that are also evident in and consistent with the AMSR-E data. Of interest is the detection of discrete areas of interior pixel melt evident in 2003 and 2005 from MODIS–MADI, which are not evident in the AMSR-E retrievals. Whether this is an artefact of the melt threshold used (as pixels are only observed to be melting for periods <2 days) or actual melt response at higher elevations is uncertain.

3.3 *Comparison of temporal trends in melt area in the MODIS and AMSR-E data*

Figure 3 details a direct melt area comparison between the two approaches. For the MODIS–MADI technique, the melt area estimates for all year, with the exception of 2005, are within 5–10% of each other. There is a slightly increasing melt trend between 2002 and 2004, before a notable increase in 2005. The AMSR-E XPGR approach, on

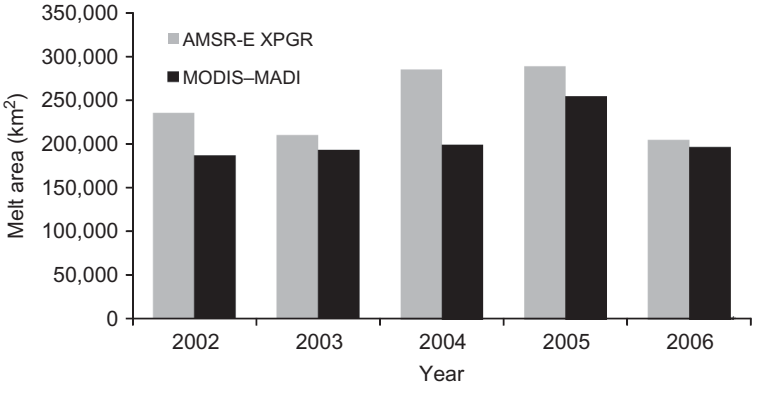

Figure 3. Comparison of melt area (km^2) between 2002 and 2006 using AMSR-E XPGR with a threshold of –0.025 (grey) and MODIS–MADI with a threshold of 65 (black).

the contrary, shows more variability, with 2004 and 2005 representing years of highest melt and 2003 and 2006 displaying the lowest melt (and best agreement with the MODIS–MADI). Considering that the approaches represent quite different physical mechanisms and penetration depths (see table 1), the trends appear to be relatively consistent. For 2004, the difference can possibly be explained by the higher number of pixels present in the XPGR approach that indicate melt durations of less than 5 days (red-orange bands in figure 2). This represents approximately 1–3% of the AMSR-E observation record – a melt period of relatively small duration considering the temporal consistency of the AMSR-E data. This spatial feature is interesting because such a large region of melt, corresponding to such a short period, is not apparent in other years of XPGR retrievals. Whether this response is observed in other microwave-based sensors such as SSM/I remain to be determined, as little has been published to date reflecting this period. However, it is not unexpected that different algorithms will identify differences in melt response. Recent efforts by Ashcraft and Long (2006) in comparing six different microwave- and scatterometer-based approaches identified that significant melt can occur without meeting XPGR melt-detection requirements. The same result is quite possible for the MADI technique, highlighting the need for an integrative approach to melt detection.

Overall, there is good agreement between the low-resolution AMSR-E XPGR retrievals and the newly developed high-resolution MODIS–MADI. Both techniques represent complementary approaches to detecting melt onset and melt area over the Greenland ice sheet. Unfortunately, the advantage of the spatial detail that is accessible from remote platforms is also a limiting factor in determining accuracy because independent validations of such observations cannot be obtained other than at a few locations. The lack of *in situ* measurement with which to evaluate such techniques highlights the importance of developing an integrated assessment of melt response using available Earth observation resources. Integrating MODIS and AMSR-E data together with other remote sensing approaches (Hall *et al.* 2009), as has been done in hydrological applications (McCabe *et al.* 2008), will enable enhanced assessment of melt dynamics. Such data fusion will assist in advancing modelling capacity by providing analogues to melt response predicted by current ice-sheet models and also in monitoring changes in cryospheric regions.

4. Conclusion

A novel remote sensing method based on reflected visible and near-infrared radiation that responds differently to ice, water and melting snow has been introduced. Here we evaluate the approach for the retrieval of summer melt area, focusing on a central western region of the Greenland ice sheet. Using reflectance data from the MODIS instrument, the detection has the potential to discriminate between dry and wet snow at high spatial resolutions. There is potential for retrieving information at a resolution of 500 m, increasing the capacity to detect spatial melt features well beyond the capacity of current microwave methods. The MADI approach should be useful for detecting the onset and extent of snowmelt globally, quantifying the spatiotemporal variability of ice sheets and glaciers, and for long-term monitoring of the melt area of the Greenland ice sheet. Although there is an obvious spatial advantage of higher resolution near-infrared reflectance data (potentially 500 m $\times$ 500 m) over microwave-based techniques (25 km $\times$ 25 km), the question of consistency between datasets requires further examination, as does the development of data fusion techniques to merge these sensors.

Acknowledgements

This research was supported by Los Alamos National Laboratory's Directed Research and Development Project (LDRD) entitled 'Resolving the Aerosol-Climate-Water Puzzle (20050014DR)'.

References

Abdalati, W. and Steffen, K., 1995, Passive microwave-derived snow melt regions on the Greenland ice sheet. *Geophysical Research Letters*, **22**, pp. 787–790.

Abdalati, W. and Steffen, K., 1997, Snow melt on the Greenland ice sheet as derived from passive microwave satellite data. *Journal of Climate*, **10**, pp. 165–175.

Abdalati, W. and Steffen, K., 2001, Greenland ice sheet melt extent: 1979–1999. *Journal of Geophysical Research*, **106**, pp. 33983–33989.

Ashcraft, I.S. and Long, D.G., 2006, Comparison of methods for melt detection over Greenland using passive and active microwave measurements. *International Journal of Remote Sensing*, **27**, pp. 2469–2488.

Cazenave, A., 2006, How fast are the ice sheets melting? *Science*, **314**, pp. 1250–1252.

Chylek, P. and Borel, C., 2004, Mixed phase cloud water/ice structure from high spatial resolution satellite data. *Geophysical Research Letters*, **31**, doi: 10.1029/2004GL020428.

Chylek, P., McCabe, M., Dubey, M.K. and Dozier, J., 2007, Remote sensing of Greenland ice sheet using multispectral near-infrared and visible radiances. *Journal of Geophysical Research D: Atmospheres*, **112**, doi: 10.1029/2007JD008742.

Fettweis, X., Van Ypersele, J.-P., Gallée, H., Lefebre, F. and Lefebvre, W., 2007, The 1979–2005 Greenland ice sheet melt extent from passive microwave data using an improved version of the melt retrieval XPGR algorithm. *Geophysical Research Letters*, **34**, L05502, doi: 10.1029/2006GL028787.

Hall, D.K., Nghiem, S.V., Schaaf, C.B., Digirolamo, N.E. and Neumann, G., 2009, Evaluation of surface and near-surface melt characteristics on the Greenland ice sheet using MODIS and QuikSCAT data. *Journal of Geophysical Research*, **114**, F04006, doi:10.1029/2009JF001287.

Hall, D.K., Riggs, G.A., Salomonson, V.V., Digirolamo, N.E. and Bayr, K.J., 2002, MODIS snow-cover products. *Remote Sensing of Environment*, **83**, pp. 181–194.

Hanna, H., Huybrechts, P., Janssens, I., Cappelen, J., Steffen, K. and Stephens, A., 2005, Runoff and mass balance of the Greenland ice sheet: 1958–2003. *Journal of Geophysical Research*, **110**, D13108, doi: 10.1029/2004JD005641.

Jackson, J., 1975, *Classical Electrodynamics* (New York: John Wiley and Sons).

Joughin, I., Abdalati, W. and Fahnestock, M., 2004, Large fluctuations in speed on Greenland's Jakobshavn Isbrae glacier. *Nature*, **432**, pp. 608–610, doi: 610.1038/nature03130.

McCabe, M.F., Wood, E.F., Wojcik, R., Pan, M., Sheffield, J., Gao, H. and Su, H., 2008, Hydrological consistency using multi-sensor remote sensing data for water and energy cycle studies. *Remote Sensing of Environment*, **112**, pp. 430–444.

Mote, T.L., 2007, Greenland surface melt trends 1973–2007: evidence of a large increase in 2007. *Geophysical Research Letters*, **34**, L22507, doi:10.1029/2007GL031976.

Nghiem, S.V., Steffen, K., Neumann, G. and Huff, R., 2005, Mapping of ice layer extent and snow accumulation in the percolation zone of the Greenland ice sheet. *Journal of Geophysical Research*, **110**, F02017, doi: 10.1029/2004JF000234.

Rennermalm, A.K., Smith, L.C., Stroeve, J.C. and Chu, V.W., 2009, Does sea ice influence Greenland ice sheet surface-melt? *Environmental Research Letters*, **4**, 024011, doi: 10.1088/1748-9326/4/2/024011.

Ringot, E. and Kanagaratnam, P., 2006, Changes in the velocity structure of the Greenland ice sheet. *Science*, **311**, pp. 986–990, doi: 910.1126/science.1121381.

Steffen, K. and Huff, R., 2005, Greenland melt extent, 2005. Available online at: http://cires.colorado.edu/science/groups/steffen/greenland/melt2005/ (accessed 1 May 2010).

Steffen, K., Nghiem, S.V., Huff, R. and Neumann, G., 2004, The melt anomaly of 2002 on the Greenland ice sheet from active and passive microwave satellite observations. *Geophysical Research Letters*, **31**, L20402, doi: 10.1029/2004GL020444.

Tedesco, M., Serreze, M. and Fettweis, X., 2008, Diagnosing the extreme surface melt event over southwestern Greenland in 2007. *The Cryosphere*, **2**, pp. 159–166.

Thomas, R.H., Abdalati, W., Frederick, E., Krabill, W.B., Manizade, S. and Steffen, K., 2003, Investigation of surface melting and dynamic thinning on Jakobshavn Isbrae, Greenland. *Journal of Glaciology*, **49**, pp. 231–239.

Ulaby, F.T., Moore, R.K. and Fung, A.K., 1982, *Microwave Remote Sensing II: Radar Remote Sensing and Surface Scattering and Surface Emission Theory*, pp. 1065–2162 (Dedham, MA: Artech House).

Ulaby, F.T., Moore, R.K. and Fung, A.K., 1986, *Microwave Remote Sensing III: From Theory to Applications*, pp. 1065–2162, pp. 1120 (Dedham, MA: Artech House).

Velicogna, I. and Wahr, J., 2006, Acceleration of Greenland ice mass loss in spring 2004. *Nature*, **443**, pp. 329–331, doi: 310.1038/nature05168.